iJRASET
International Journal For Research in Applied Science and Engineering Technology



INTERNATIONAL JOURNAL FOR RESEARCH

IN APPLIED SCIENCE & ENGINEERING TECHNOLOGY

Volume: 11 **Issue:** III **Month of publication:** March 2023

DOI: https://doi.org/10.22214/ijraset.2023.49572

www.ijraset.com

Call: 08813907089 | E-mail ID: ijraset@gmail.com

International Journal for Research in Applied Science & Engineering Technology (IJRASET)
ISSN: 2321-9653; IC Value: 45.98; SJ Impact Factor: 7.538
Volume 11 Issue III Mar 2023- Available at www.ijraset.com

Transmission of Power and Signal Multiplex for Electric Vehicles Using Cascaded Multilevel Inverters

Mrs. K. Ramya[1], S. Hemasri[2], Y. Naveen[3], K. Veeresh[4], B. Sirisha[5], M. Merisha[6]
[1]*Assistant Professor, Department of EEE, Sree vahini institute of science and technology., Tiruvuru., NTR District., AP, India*
[2, 3, 4, 5, 6]*UG scholar students Sree vahini institute of science and technology.,Tiruvuru.,NTR District., AP, India*

Abstract: ***P&SMT, or power and signal multiplex transmission, is a method for transmitting communication signals using power electronic circuits. A three-phase cascaded multilevel inverter-based P&S MT system is recommended in this investigation. By allowing communication signals to be transmitted without utilizing a Controller Area Network bus, the proposed solution can lower the wiring expense of the existing electric vehicle (EV) communication system. The system's architecture enables battery balancing discharge and motor speed management for EVs. In a simulation system proposed in MATLAB/Simulink, both power and communication signals are effectively conveyed using the combined pulse width modulation scheme and frequency shift keying approach. The maximum signal rate of the proposed system is established at 600 bits per second by analyzing the bit error rate of the sent signal.***

Index Terms: ***Three-phase DC-AC converter, frequency shift keying, battery capacity of charge, controller area network, and motor speed control.***

I. INTRODUCTION

The energy mix that was used to create power on each day and throughout each time slot was retrieved using the data from the Italian national grid operator (Terna). The third phase involved obtaining emission factors for greenhouse gas (CO2) and pollutant emissions using various power-generating mixtures (CO, NOx, HC, and particulate). The emission factors in g/km were determined using data on the electric usage of cars registered in Rome and compared to the constraints established by European regulation for conventional vehicles (gasoline and diesel) Because they don't release pollutants into the environment, electric vehicles (EVs), which are propelled by electric motors, are growing in popularity today. The noise level of EVs is significantly lower than that of conventional internal combustion engine vehicles (ICEVs) due to the absence of internal combustion engine noise and its masking effect in EVs, as illustrated in Figure 1a. In addition, compared to ICEVs, the aerodynamic noise and road noise contribution to the interior noise in EVs is high. [1,2].

Moreover, recharging an EV battery at night can help the grid balance the load and save expenses by preventing the peak in power consumption [3]. According to findings, 39.2% of all emissions in 2007 came from vehicles. Since emissions must be drastically reduced if humans are to prevent a catastrophic greenhouse effect, governments around the world have adopted strict emission regulations.

For instance, the Emission Standard of Automobiles of Europe IV Standard has been in effect in Europe since 2005.

The government also implemented fuel duty levy levies, which, together with increasing crude oil prices, result in higher fuel costs. Thus, the automobile industry is compelled by law to create electric vehicles (EVs) with great fuel efficiency and minimal emissions.

A road vehicle that uses electric propulsion is known as an EV. The emerging clutch less automated manual gearboxes for battery electric vehicles and other powertrain systems for hybrid electric vehicles are examined in this research, along with several types of motor speed synchronization control methods [4]- [5]. Because of its high reliability and high connectivity baud rate, using a Controller Area Network (CAN) bus for data transfer in electric vehicles is one of the methods that is widely accepted by manufacturers and researchers [6]-[7]. Fig. 1 depicts the general layout of an EV's powertrain. For a 2-level inverter, several conventional power systems for EVs use a DC/DC converter to enhance the battery voltage [8]- [9]. This methodology may lead to substantial switching losses due to its rapid voltage change rates (dV/dt). Due to the use of large inductors for the DC/DC boost converters, such a system is both costly and has a low power density.

©IJRASET: All Rights are Reserved

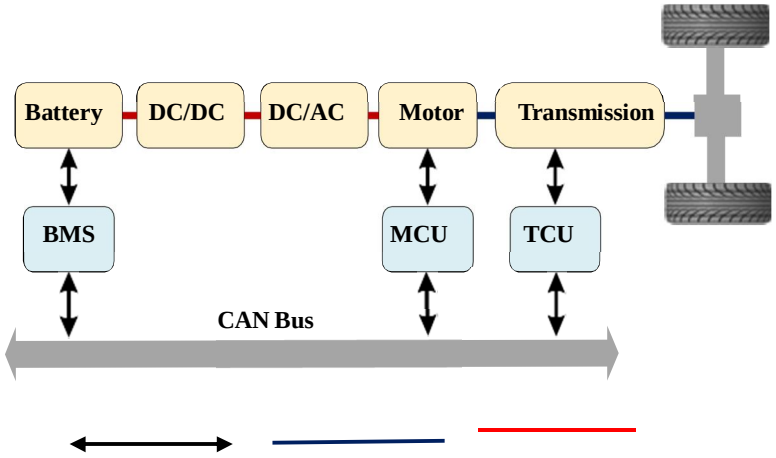


Figure 1: shows how an EV's main powertrain is constructed.

Traditional EVs use the CAN bus to achieve their internal communication, but the power transmission line and the communication channel are still two separate parts of the system that may still be optimized. In order to transfer power and communication signals simultaneously through a three-phase multilevel inverter circuit for EVs, the power and signal multiplex transmission (P&SMT) approach is suggested in this research. A DC/DC converter is not necessary since the cascaded multilayer inverter itself may increase the battery voltage because the individual components of the multilevel inverter have substantially lower switching losses than those of a 2-level inverter. In the suggested system, frequency shift keying (FSK) is used to modify the transmitted signals, while pulse width modulation (PWM) is used to convert power.

The suggested solution can significantly lower the cost of the communication system since the power and signals are sent concurrently rather than using a CAN bus as a communication channel in modern EVs by using the same power line. The rest of this essay is arranged as follows: A few pertinent pieces of P&SMT literature are reviewed in Part II. The suggested system's structure and P&SMT methods are described in Part III. Part IV presents the simulation findings. A brief conclusion is drawn in Section V at the end of this study.

II. A REVIEW OF THE RESEARCH PROJECT WORK

Power Line Communications aggregates a wealth of knowledge on PLC-specific subjects that gives the reader a comprehensive study of the key milestones in the industry. collects material that is widely spread in contemporary literature, including research papers and standards, and serves as a single-source reference manual for PLC. includes both current research issues and state-of-the-art themes [10]. Adding signals to a power line might make the channel more difficult because the power line itself is not intended to transport communication data. A broadband power line communication (PLC) model should also take electromagnetic interference into account since its 2 MHz to 32 MHz carrier frequency may be the same as the frequency of short-wave radios [11]. Power over Ethernet (PoE) is a method that enables various IP-based terminals, such voice-over-Internet telephones and IP cameras, to deliver both data and electric power via twisted-pair Ethernet cable [12]. Nevertheless, this strategy is not acceptable for pan-tilt-zoom cameras and other high-power-demanding applications [13].

Since the maximum output power of power sourcing equipment for PoE is larger than 15.4 W in the standard IEEE 802.3af.13. It will be crucial to continue to (a) quantitatively assess the levels of RF emissions from everyday household items and smart meters to which the public may be exposed and (b) investigate the potential thermal and non-thermal effects of such RF emissions on human health as the use of wireless technologies of all kinds increases. If customers are still concerned about wireless meters, an alternate smart meter configuration (such as one that is connected) might be taken into account. In addition to the advantages, PLC technology offers built-in security [14]. In the past few years, solutions for utilizing power electronic circuits for signal transmission have been studied. In the literature [15]– [17], the signal transmission function during power conversion is realized using the Buck circuit with a multipath load structure. The switching ripple created on the input bus may be modulated with the FSK approach by altering the switching frequency with the PWM technique. In their studies, the switching signal is captured using a peak detection circuit, and the digital "0" and "1" are then identified using band-pass filtering and signal processing [18]-[19]. Bidirectional signal

transmission between a master module and slave modules is accomplished in their design. Power and signal are transmitted sequentially over a single topology because separate switches work with varying duty ratios, and the transmitted signals are abstracted by detecting changes in the bus voltage. Yet, because of the intermittent transmission of signals, such a system has a poor communication rate.

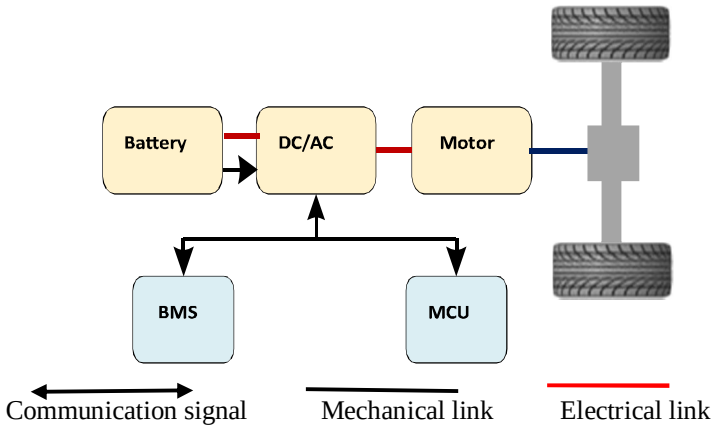


Figure 2. The suggested system architecture for an EV employing the P&SMT approach is shown.

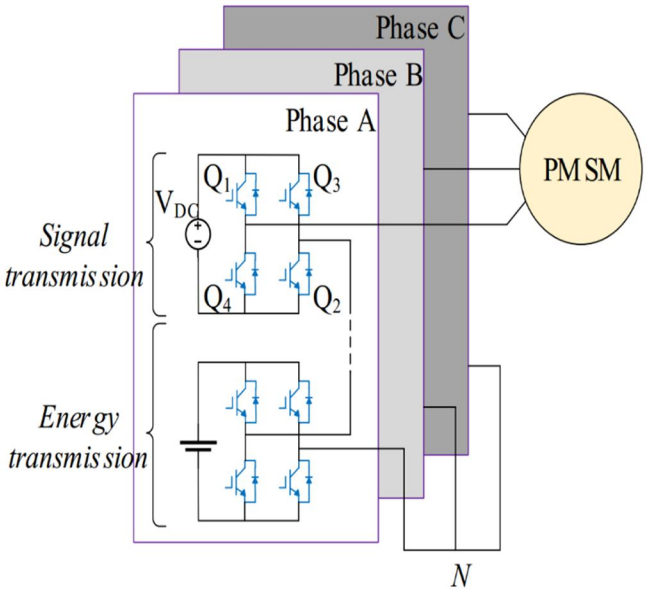


Fig.3 shows the suggested P&SMT system for electric vehicles.

III. PROPOSED TRANSMISSION OF POWER AND SIGNAL MULTIPLEX

A. System Architecture

In this article, the transmitted battery state of charge (SOC) signal and the motor speed control signal are used as illustrations to further explain the foundations of the proposed P&SMT approach. Fig. 2 depicts the preferred system architecture for an EV adopting the P&SMT approach. Signals are sent through a three-phase multilevel inverter circuit to enable communication between the battery and BMS, as well as between the MCU and motor. Fig. 3 shows the recommended structure of a three-phase P&SMT system. Each phase of the inverter architecture is made up of four series-connected H-bridge cells, one of which is driven by a DC voltage source and is used for signal transmission, while the other three are battery-powered and are used for energy transmission. tempo of the motor the phase A and phase B sections are used to deliver the speed adjustment signal and the SOC signal, respectively. In this scenario, the inverter's load is a permanent magnet synchronous motor (PMSM).

B. Transmission of Signals

In the proposed methodology, the signals are modulated using the FSK mechanism, and the signal transmission scheme is shown in Fig. 4. Two carriers with different frequencies, as illustrated in SC, can be used to modulate digital bits "1" and "0," respectively, if the transmitted 4-bit signal SI is "1010". The signal may be modified by manipulating the quick swapping of the four switches in the cell since it is intended to be relayed through an H-bridge cell in each phase. A switch will specifically turn on if a gate signal of digital '1' is applied and turn off if a gate signal of digital '0' is applied. The switches Q1 and Q2 in Fig. 3 function together and at the same instance, switches Q3 and Q4 both turn on and off. Also, to prevent a short circuit, switches Q1 and Q2 work in the opposite state from switches Q3 and Q4. Because the three other cells used for energy transmission are coupled in series with the H-bridge cell used for signal transmission, The output current waveform can be thought of as being overlaid with the transmitted signal.

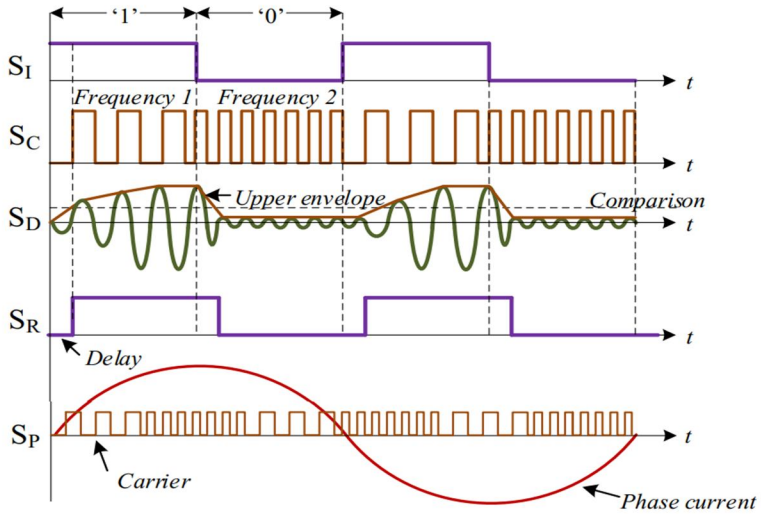


Fig. 5 The signal transmission scheme of the proposed system is represented by SI, which is the initial 4-bit signal "1010," SC, the carrier waveform, SD, the extracted carrier for the digital "1," after applying a band-pass filter, SR, the restored signal, and SP, which is the output phase current waveform superimposed with the signal's carrier.

The Band-pass filter is extracted to transmit the signal with in the current receiving output waveform. Any signal has the f(x) and the time period T and angular frequency $\omega = 2\pi/T$, its was expressed in Fourier expansion form.

$$F(x) = \frac{1}{2}a_0 + \sum_{n=1}^{\infty}(a_n \cos n\omega x + b_n \sin n\omega x \quad (1)$$

Where the coefficients $a_0, a_n, and\ b_n$ in this series are defined by

$$\left\{\begin{array}{c} a_0 = \frac{2}{T}\int_{-\frac{T}{2}}^{\frac{T}{2}} f(x)dx \\ a_n = \frac{2}{T}\int_{-\frac{T}{2}}^{\frac{T}{2}} f(x)\cos n\omega x dx \\ b_n = \frac{2}{T}\int_{-T/2}^{T/2} f(x)\sin n\omega x dx \end{array}\right\} \quad (2)$$

Similarly, if a square wave f(t) with time period T is applied as a carrier for digital '1', it can be expressed as

$$f(t) = \left\{\begin{array}{c} 0\ -\frac{T}{2} \le t < 0 \\ 1\ 0 \le t \le \frac{T}{2} \end{array}\right\} \quad (3)$$

The Fourier series expansion of f(t) is derived as

$$F(t) = \frac{1}{2} + \frac{2}{\pi}\sin x + \frac{2}{3\pi}\sin 3x + \frac{2}{5\pi}\sin 5x + \frac{2}{7\pi}\sin 7x + \ldots + \frac{2}{n\pi}\sin nx \quad (4)$$

©IJRASET: All Rights are Reserved

n being an odd number. First-order harmonics can be used to restore communication signals since they have the maximum amplitude in the Fourier series expansion of f(t), which only comprises the odd harmonic components. As an illustration, the curve SD in Fig. 4 depicts an envelope detector can be used to obtain the upper envelope of the digital "1" demodulated carrier. When the upper envelope's amplitude exceeds the comparison value and a suitable comparison value is used, the upper envelope can be recovered to digital 1.

Otherwise, a digital "0" will be retrieved. After sampling the recovered digital signal at the SI's initial bit rate, the restored SR is finally acquired.

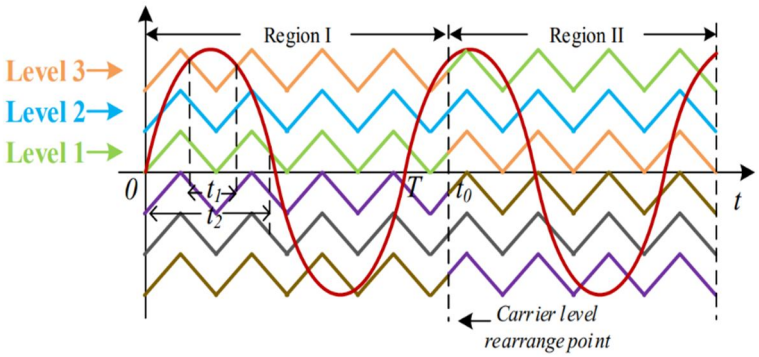


Fig.6 Rearrangement at the carrier level during PWM

C. Motor speed Regulation

Optimizing Motor Speed and Battery Balance Discharging In the proposed technique, the power frequency is modulated together with the broadcast signal to control the motor speed. The link between a PMSM's motor speed n, pole-pair p, and power frequency f is explicitly shown as

$$n = \frac{60f}{p} \tag{5}$$

where 60 symbolizes the rate in seconds per minute. A 2-pole pair motor's speed should theoretically fluctuate between 1200 and 1800 r/min if the power frequency ranges between 40 and 60 Hz. The power frequency f is then computed using the transmitted signal s using the formula.

$$f = 20 \times s + 40 \tag{6}$$

If the transmitted signal contains a digital '0' or '1', the power frequency will be 40 Hz or 60 Hz, respectively. The three-phase reference sinusoidal waves are then created using the equations Pa, Pb, and Pc, where Pa stands for phase A, Pb for phase B, and Pc for phase C, respectively, and A represents the amplitude. The phase A reference wave is 2/3 and 4/3 radians behind the phase B and phase C reference waves, respectively. Lastly, the motor is driven by modulated variable-frequency sine waves to alter the motor speed.

$$\left\{\begin{array}{c} P_a = A\sin(2\pi f) \\ P_b = A\sin\left(2\pi f - \frac{2}{3}\pi\right) \\ P_c = A\sin(2\pi f - \frac{4}{3}\pi) \end{array}\right\} \tag{7}$$

The gating signal of a switch is generated using the conventional sinusoidal PWM method by comparing the reference wave with a triangular carrier. The duty cycle of each switch varies because different carriers and the reference wave intersect at distinct locations. For instance, as shown in Fig., a switch controlled by a "Level 3" carrier has a lower duty cycle than a switch modulated by a "Level 1" carrier (t1) for a brief period. Hence, by periodically rearranging the carrier levels inside the PWM process, the battery balance discharge may be achieved.

Table-1 Parameters Used in The Suggested System

Parameter name	value
DC voltage source	30V
Battery voltage	48V
PWM carrier frequency	2kHz
PWM Referenced sine wave frequency	40 Hz,60 Hz
Carrier frequency of motor speed adjustment signal	4 kHz for '1' and 8 kHz for '0'
Carrier frequency of SOC signal	6 kHz for '1' and 10 kHz for '0'

IV. SIMULATION RESULTS AND ANALYSIS

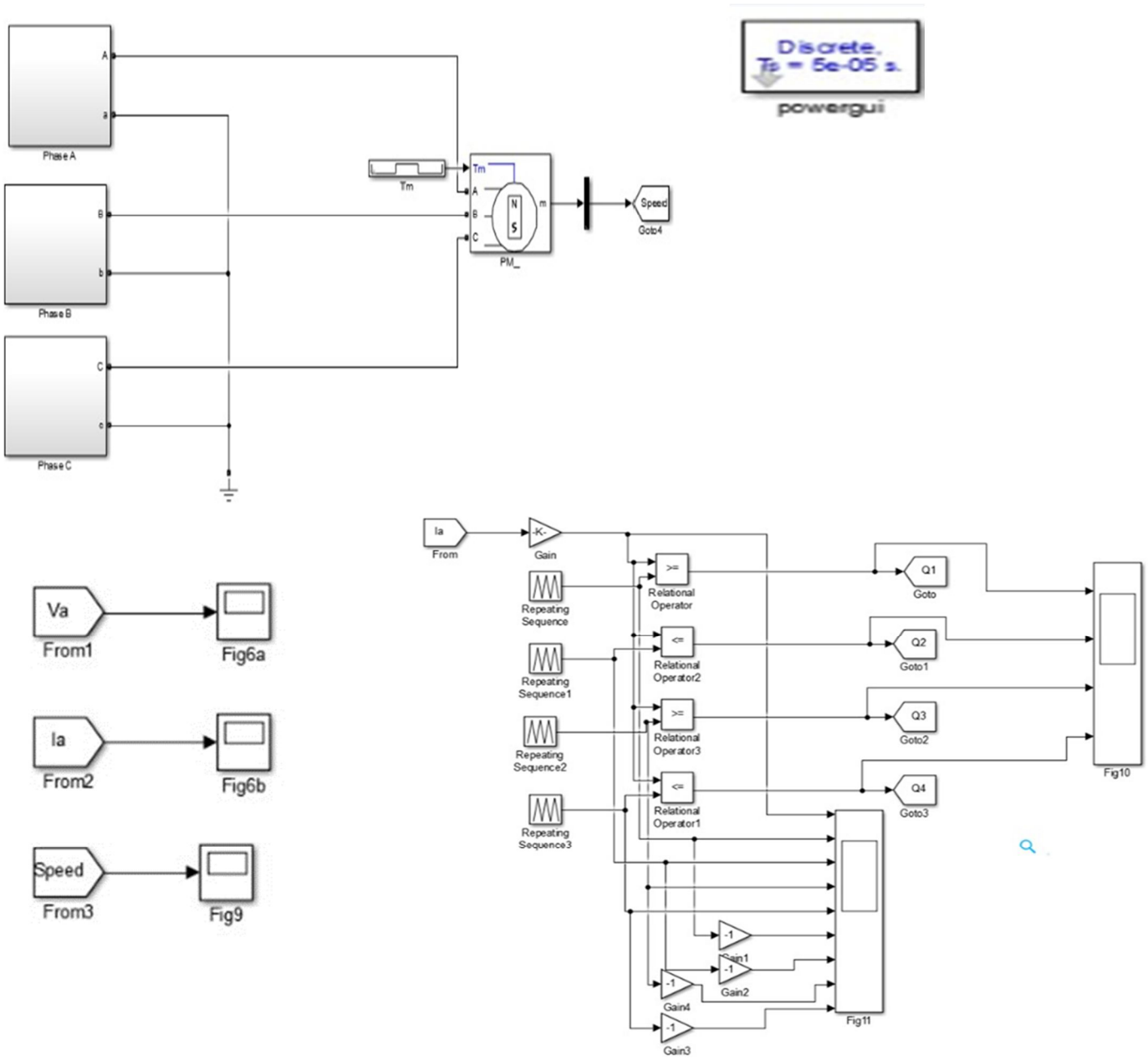


Fig. 8 simulink diagram of the cascaded multilevel inverter Based P&SMT for EV

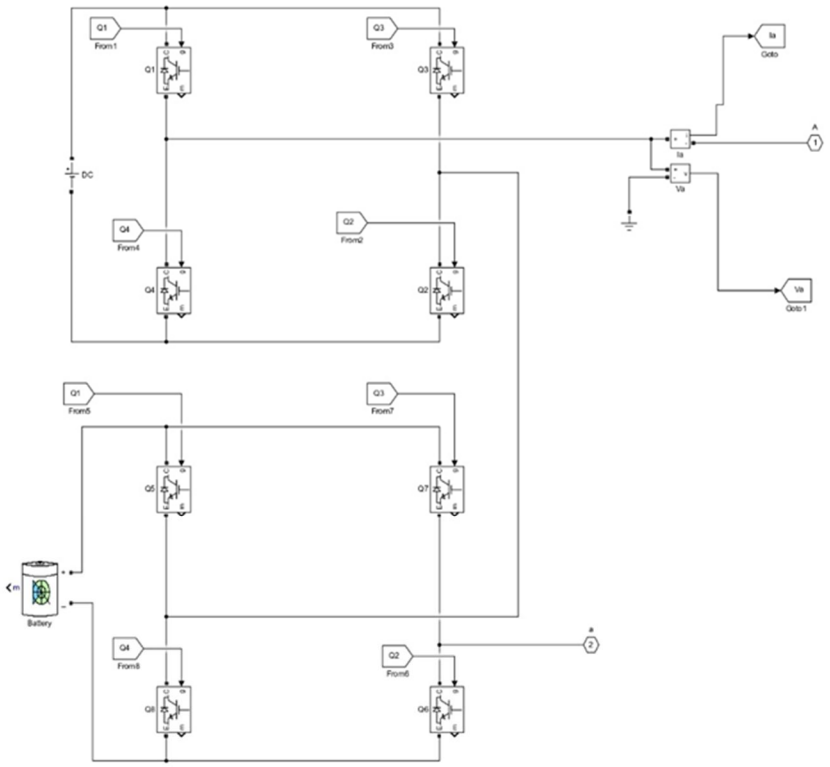


Fig. 9 cascaded H-Bridge(Two cell) multi-level inverter

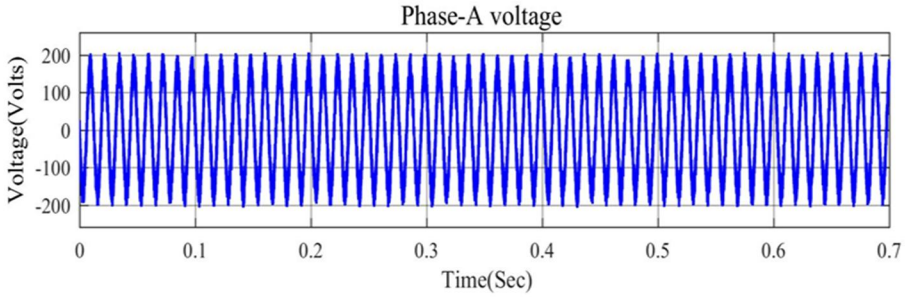


Fig. 10 The output voltage waveform of phase A

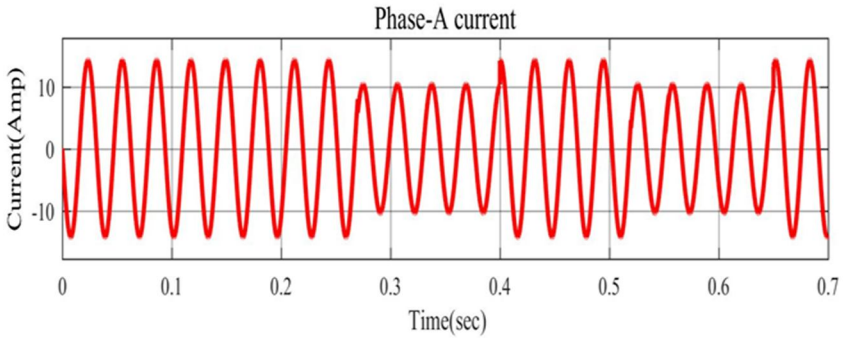


Fig. 11 the output current waveform of phase A

©IJRASET: All Rights are Reserved | SJ Impact Factor 7.538 | ISRA Journal Impact Factor 7.894 |

As contrasted to a switch operating with a wider duty cycle, the switch with a reduced duty cycle uses less energy. Consequently, once the system has been working for a while, it may transpire that the batteries' remaining capacity is out of balance. Hence, by periodically rearranging the carrier levels inside the PWM process, the battery balance discharge may be achieved. To accomplish this goal, a data stream created from the battery SOC values at the periodic sampling point is first communicated via the FSK technique through a full-bridge cell supplied by a DC voltage source. The SOC values are split into various decimal numbers once the signal from the phase current has been demodulated. Lastly, the transmitted SOC values are used to reorder the PWM carrier levels, and the battery balance discharge is accomplished.

The first set of simulation parameters and output waveforms

A. Changes in the Motor Speed Transfer of Signals

The transmission rate of the signal is 100/3 bps since the original 8-bit motor speed adjustment signal is configured as 11110000 with 0.03 s per bit. Next, to distinguish between two adjacent 8-bit data strings, a 4-bit cyclic redundancy code (CRC) is inserted at the end of each data string. The full 12-bit data frame is 111100000100 since the 4-bit CRC code produced by the generator polynomial is 0100. By using the modulo-2 division method and the divisor 11110 to divide the sent data frame, the system may check to see whether the residual is zero to see if the frame data is incorrect. If it is 0, it demonstrates that there were no transmission faults in the frame data; if not, there was a problem. The first message includes information as well as Fig. 1 displays the message data after the CRC coding. It's important to note that the time required to send a frame with and without a CRC code is the same; as a result, the 12-bit data is delivered at a rate of 0.02 s per bit. The 4 kHz square wave is utilized as a carrier for digital "1," and the 8 kHz square wave is used as a carrier for digital "0," once the whole data frame has been collected. The 4 kHz carrier is then recovered from the phase current waveform with a band-pass filter after the signal has passed through an H-bridge cell. The transmitted signal is then recovered using an algorithm using the filtered carrier waveform SF in Fig 12.

$$20\log x = -6 \tag{8}$$

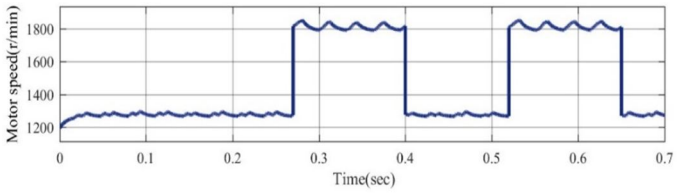


Fig.12 The sent 8-bit signal, "11110000," which controls the motor speed.

In other words, the waveform SF's amplitude in the zone of cut-off frequencies (0.04) is half that of the region of passband frequencies (0.08). As a result, "0.05" is chosen to distinguish between the passband frequency area and the cut-off frequency region of the filtered wave. There is a delay in the recovered signal SST in Fig. 4, which is mostly brought on by the filtering procedure, as compared to the waveform SE in Fig. 3. The recovered signal SRE in Fig. 4 is produced when the 4-bit CRC coding is removed after each 8-bit data frame. The transmitted data in the first period before the 4-bit CRC code is 'ignored' by the system because the 4-bit CRC code first appears at 0.18 s (0.028+ 0.02 (one-bit delay) = 0.18). Also, the pace of the recovered data frame is comparable to that of the original signal (0.03 s per bit). Although SRE may be seen as delaying a full signal period plus one sampling time, the recovered 8-bit data frame first emerges at 0.27 s (0.038+ 0.03 (one-bit delay) = 0.27).

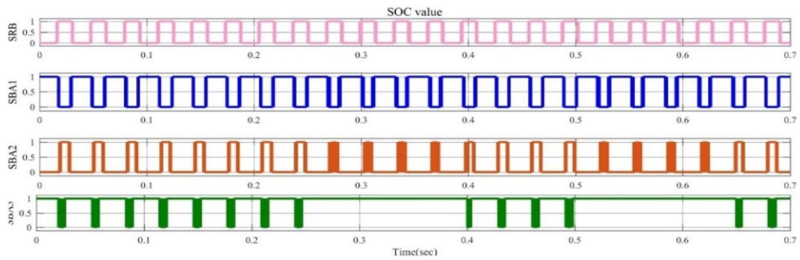


Fig.9 Three SOC frames together make up the code string known as SCB.

The recovered SOC signal is termed SRB; SBA1 includes the frame '01100100', which denotes the SOC of the first battery; SBA2 contains the frame '00101000," and SBA3 contains the frame '00100011', which denotes the SOC of the second battery. Lastly, the motor speed is controlled by the signal SRE that was retrieved in Fig. 5 and whose waveform is shown in Fig. 6. The motor speed varies every time the signal shifts from '0' to '1' for around 0.01 seconds. The motor speed stabilizes between 1200 r/min and 1800 r/min as predicted because the power frequency is made to fluctuate between 40 Hz and 60 Hz. Considering that the transmitted signal is superposed on the energy-based phase current, The phase current waveform will be disrupted by the signal, which will impair the stability of the motor speed. The steady-state volatility of the motor speed is also higher than that of the usual double closed-loop control technique because the motor speed is open-loop governed by varying the motor power ***frequency.***

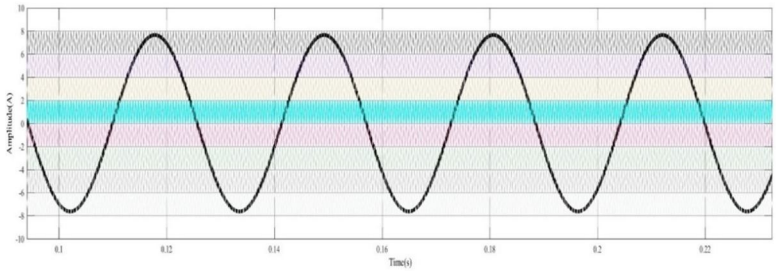


Fig. 10 The Reference sinusoidal wave and the rearranged carriers employed in PWM.

B. Capacity for System Data Transfer

Calculating the error rate of the sent signal will reveal the proposed system's maximum data transmission rate. The error rate of the sent signal is estimated by contrasting the original data string with the one received one bit at a time. The link between the bit rate and the error rate is demonstrated by progressively raising the speed of the motor speed control signal. According to this number, the error rate starts to increase when the signal rate exceeds 600 bit/s. There is a very high demand for the accuracy of the communicated data since the proposed system controls the battery discharge process in accordance with the batteries' SOC value. As soon as the demodulated data is inaccurate, the battery's SOC sequencing fails to be anticipated outcomes. Comparing this system's data rate to more traditional communication methods like optical fiber reveals that it is rather low. Yet, this system can handle such a modest data rate since the batteries' SOC value does not change considerably quickly. Furthermore, a data rate of 600 bit/s is adequate to convey the motor speed control signal since the motor speed requires some time to settle after each frequency change.

V. CONCLUSION

It is recommended that a three-phase, multilevel inverter-based P&SMT system be used to control the motor speed and discharge the battery balance for EVs. Each phase of the inverter architecture involves four series-connected H-bridge cells, three of which are controlled by PWM for energy transmission and the other two by FSK for signal transmission. The complexity of the overall system can be decreased by simplifying the system wiring since the suggested technique uses a portion of the power electronic circuit as a communication channel. The viability of the hypothesized P&SMT technique is tested by sending the battery SOC signal and the motor speed adjustment signal through the phase-A and phase-B currents, respectively, using a simulation model developed in MATLAB/Simulink. The signal transmission also After examining the connection between the signal bit rate and error rate, the capacity of the suggested approach is found to be 600 bit/s.

REFERENCES

[1] T. Donateo, F. Licci, A. D'Elia, G. Colangelo, D. Laforgia and F. Ciancarelli, "Evaluation of emissions of CO2 and air pollutants from electric vehicles in italian cities," Applied Energy, vol. 157, pp. 675-687, Nov. 2015.
[2] C. Ma, C. Chen, Q. Liu, H. Gao, Q. Li, H. Gao, and Y. Shen, "Sound quality evaluation of the interior noise of pure electric vehicle based on neural network model," IEEE Transactions on Industrial Electronics, vol. 64, no. 12, pp.9442-9450, 2017.
[3] M. Yilmaz and P. T. Krein, "Review of the impact of vehicle-to-grid technologies on distribution systems and utility interfaces," IEEE Transactions on Power Electronics, vol. 28, no. 12, pp. 5673-5689, 2013.
[4] K.Ç. Bayindir, M.A. Gözüküçük and A. Teke, "A comprehensive overview of hybrid electric vehicle: Powertrain configurations, powertrain control techniques and electronic control units,"Energy conversion and Management, vol. 52, no. 2, pp. 1305-1313, 2011.
[5] X. Zhu, H. Zhang, J. Xi, J. Wang, and Z. Fang, "Optimal speed synchronization control for clutch less AMT systems in electric vehicles with preview actions," 2014 American Control Conference, pp. 611-4616, 2014.

[6] F. Zhou, S. Li, and X. Hou, "Development method of simulation and test system for vehicle body CAN bus based on Canoe," 2008 7th World Congress on Intelligent Control and Automation, pp. 7515-7519, 2008.
[7] M. Zheng, B. Qi, and H. Wu, "A li-ion battery management system based on CAN-bus for electric vehicle," 2008 3rd IEEE Conference on Industrial Electronics and Applications, pp. 1180-1184, 2008.
[8] L. M. Tolbert, F. Z. Peng and T. G. Haberle, "Multilevel inverters for electric vehicle applications," Power Electronics in Transportation (Cat. No.98TH8349), pp. 79-84, 1998.
[9] Z. Du, B. Opanci, L. M. Tolbert and J. N. Chiasson, "DC–AC cascaded H-bridge multilevel boost inverter with no inductors for Electric/Hybrid electric vehicle applications," IEEE Transactions on Industry Applications, vol. 45, no. 3, pp. 963-970, 2009.
[10] L. Lampe, A.M. Tonelli and T.G. Swart, Power Line Communications: Principles, Standards and in Application from multimedia to smart grid, John Wiley & Sons, 2016.
[11] W. Huagang, T. R. Meng and L. S. Wen, "Measurement and analysis of electromagnetic emissions for broadband power line (BPL) communication," 2017 IEEE 5th International Symposium on Electromagnetic Compatibility (EMC- Beijing), pp. 1-4, 2017.
[12] R. V. White, "Electrical isolation requirements in power-over-ethernet (PoE) power sourcing equipment (PSE)," Twenty-First Annual IEEE Applied Power Electronics Conference and Exposition, 2006. APEC '06, pp. 4, 2006.
[13] J. Herbold, "Navigating the IEEE 802.3af standard for PoE," POWER ELECTRONICS TECHNOLOGY, vol.30, no. 6, pp. 45-48, 2004.
[14] W. Xu and W. Wang, "Power electronic signaling Technology—A new class of power electronics applications," IEEE Transactions on Smart Grid, vol. 1, no. 3, pp. 332-339, 2010.
[15] S. Saggini, W. Stefanutti, P. Mattavelli, G. Grace and M. Ghioni, "Power line communication in dc-dc converters using switching frequency modulation," Twenty-First Annual IEEE Applied Power Electronics Conference and Exposition, 2006. APEC '06, 2006.
[16] W. Stefanutti, P. Mattavelli, S. Saggini and L. Panseri, "Communication on power lines using frequency and duty-cycle modulation in digitally controlled dc-dc converters," IECON 2006 - 32nd Annual Conference on IEEE Industrial Electronics, pp. 2144-2149, 2006.
[17] W. Stefanutti, S. Saggini, P. Mattavelli and M. Ghioni, "Power line communication in digitally controlled DC–DC converters using switching frequency modulation,"IEEE Transactions on Industrial Electronics, vol. 55, no. 4, pp. 1509-1518, 2008.
[18] J. Wu, C. Li, and X. He, "A novel power line communication technique based on power electronics circuit topology," 2010 Twenty-Fifth Annual IEEE Applied Power Electronics Conference and Exposition (APEC), pp. 681-685, 2010.
[19] J. Wu, S. Zong and X. He, "Power/signal time division multiplexing technique based on power electronic circuits," 2011 Twenty-Sixth Annual IEEE Applied Power Electronics Conference and Exposition (APEC), pp. 1710-1714, 2011.
[20] C. Blake and C. Bull, "IGBT or MOSFET: Choose wisely," International Rectifier, 2001.

©IJRASET: All Rights are Reserved | SJ Impact Factor 7.538 | ISRA Journal Impact Factor 7.894 |

AUTHORS



K. Ramya obtained her Bachelor of Technology in Electrical and Electronics Engineering from Sree Rama institute of technology and science in the year 2012.she completed M. tech in Sree Rama institute of technology and science. Her areas of interests are Power Systems, Electrical Machines, Power Electronics and Devices, Electrical Circuits and Power system Analysis. Electronics and Devices.



S. Hemasri obtained her Bachelor of Technology in Electrical and Electronics from JNTUK, Tiruvuru, Andhra Pradesh, India. Her areas of interests are Power Systems, Electrical Machines, and Power Electronics and Devices.



Y. Naveen obtained his Bachelor of Technology in Electrical and Electronics from JNTUK, Tiruvuru, Andhra Pradesh, India. His areas of interests are Power Systems, Electrical Machines, and Power Electronics and Devices.



K. Veeresh obtained his Bachelor of Technology in Electrical and Electronics from JNTUK, Tiruvuru, Andhra Pradesh, India. His areas of interests are Power Systems, Electrical Machines, and Power Electronics and Devices.

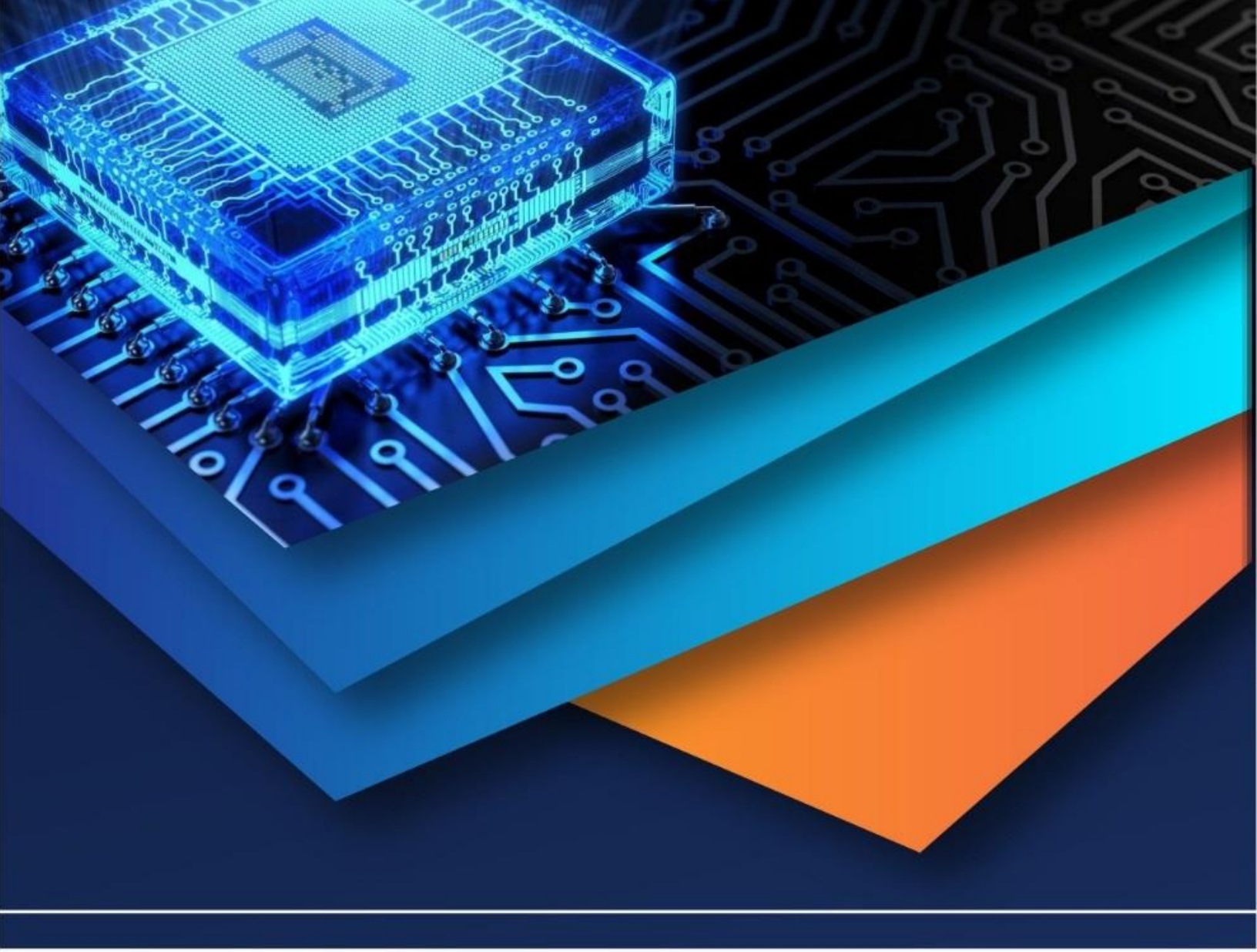


B. Sirisha obtained her Bachelor of Technology in Electrical and Electronics from JNTUK, Tiruvuru, Andhra Pradesh, India. Her areas of interests are Power Systems, Electrical Machines, and Power Electronics and Devices.



M. Merisha obtained her Bachelor of Technology in Electrical and Electronics from JNTUK, Tiruvuru, Andhra Pradesh, India. Her areas of interests are Power Systems, Electrical Machines, and Power Electronics and Devices.

©IJRASET: All Rights are Reserved | SJ Impact Factor 7.538 | ISRA Journal Impact Factor 7.894 |



10.22214/IJRASET

45.98

IMPACT FACTOR: 7.129

IMPACT FACTOR: 7.429

INTERNATIONAL JOURNAL FOR RESEARCH

IN APPLIED SCIENCE & ENGINEERING TECHNOLOGY

Call : 08813907089 (24*7 Support on Whatsapp)